# A Decentralized Control of Partitioned Power Networks for Voltage Regulation and Prevention Against Disturbance Propagation

Hasan Mehrjerdi, Serge Lefebvre, Maarouf Saad, *Senior Member, IEEE*, and Dalal Asber

***Abstract*—This paper investigates a secondary voltage control based on a graph partitioning method. The method divides the power system into regions to eventually prevent the propagation of disturbances and to minimize the interaction between these regions. The optimized number of regions is found based on the bus voltage sensitivity to disturbances being applied to loads in each region. Then, a number of representative buses are labelled as pilot buses displaying the critical point for voltage control in each region. The control uses decentralized controllers to eliminate voltage violations resulting from load variations and disturbances in the system. The decentralized controllers are implemented by fuzzy logic which is trained via offline simulations; they inject required reactive power into the regions to correct voltage violations. The methodology is applied to the IEEE 118-bus network. The results show the performance and ability of graph partitioning and fuzzy secondary voltage control to regulate the voltage and to avoid propagation of disturbances between regions.**

***Index Terms*—Fuzzy model and control, graph theory, pilot buses, power network, secondary voltage control.**

## I. Introduction

TODAY's power systems operate close to their limits, resulting a greater vulnerability to disturbances. Recent examples such as the blackout in North America in 2003, Italy in 2003, Greece in 2004 and in European countries on November 4, 2006 are representative of this vulnerability. To withstand outages/blackouts, the power industry is investing to protect its network against different disturbances, but large interconnected power systems require innovative solutions to make these practical. Although the literature presents several studies on this problem, the unique networks of Hydro-Quebec and of Canadian utilities have specific challenges. In Canada, transmission systems have long lines with loads remote from production. It is generally difficult to maintain constant voltage when the demand varies under highly loaded conditions. Without control, the voltage will exceed its operating range. This is harmful to quality and security.

Manuscript received March 16, 2012; revised June 04, 2012 and August 28, 2012; accepted October 06, 2012. Date of publication November 27, 2012; date of current version April 18, 2013. Paper no. TPWRS-00222-2012.

H. Mehrjerdi, S. Lefebvre, and D. Asber are with the Research Institute of Hydro-Quebec, Power Systems and Mathematics, Varennes, QC, Canada (e-mail: mehrjerdi.hasan@ireq.ca).

M. Saad is with the Department of Electrical and Computer Engineering, Quebec University (ETS), Montréal, QC, Canada (e-mail: maarouf.saad@etsmtl.ca).

Color versions of one or more of the figures in this paper are available online at http://ieeexplore.ieee.org.

Digital Object Identifier 10.1109/TPWRS.2012.2225154

This motivates us to study and find efficient and secure voltage regulation for power systems by controls suitable to real-time and large networks. The goal is to maintain voltages within the ranges prescribed, at all buses, following a change in the operating conditions. Voltage control means to regulate voltage profile by adjusting automatically reactive power control devices.

The primary objective of secondary voltage control (SVC) is to achieve better closed loop voltage regulation in power systems. Several methods to design secondary voltage controllers have been proposed [1]–[4]. The applications of coordinated voltage control have been tested and successfully used in France and Italy. Recently, much research work has been focused on the optimization of coordinating SVC [5]–[10].

Wen *et al.* [8] present an optimal coordinated voltage controller based on a model predictive control (MPC) scheme. MPC has been used in SVC to coordinate different control actions in order to maintain desired voltage profiles in emergencies at different locations. A single-stage Euler state predictor upon on the system model is employed to predict voltage performance under selected control actions.

Ma *et al.* [11] present an algorithm for optimizing the voltage control systems based on jumping genes paradigm in the format of hierarchical genetic algorithm. The advantage of this algorithm is that it finds solutions that can be used for stabilizing the voltage drop or even voltage collapse in a power system.

You *et al.* [12] present a method that divides a power system into smaller islands with consideration of fast restoration. Self-healing approach for large disturbances is considered to deal with tragic events when vulnerability analysis shows that the power system is approaching an emergency state. A load shedding scheme based on the rate of frequency decline is applied by shedding less load compared to the conventional load shedding.

Xu and Vittal [13] present an algorithm to identify a cutset for the application of a slow coherency based controlled islanding for large power system. They use controlled islanding for a corrective measure of last resort to prevent cascading outages caused by large disturbances. Generators belonging to the same slowly coherent group are integrated into a node, and a graph partition is used to divide the graph into a given number of regions.

This paper describes an alternate decentralized secondary fuzzy voltage control and fuzzy model estimation for power systems based on graph-based partitioning. Different methods have been developed for partition recognition and model reduction. The graph partitioning method, electrical distance method, time domain, and frequency domain approaches have been used in [14]–[16]. Model based approaches, related to the slow-coherency or eigenstructure decomposition are studied in [17] and [18].

The scheme proposed here separates the power system into smaller regions using graph theory with the goal to avoid cascading events. The algorithm is tested on the IEEE 118-bus network. This network is divided into regions that are designed to have minimum interaction and therefore any disturbances in a particular region will not strongly propagate to the other regions. The regions can be reconfigured and updated in accordance with variations in grid structure. In this paper, disturbances are defined as increasing of active and reactive power to the loads.

Selection of the pilot buses is the most crucial point for an appropriate controller design to obtain efficient voltage regulation. Methods have been already proposed for the choice of pilot buses [19], [20]. The selection of pilot buses in the paper is based on the largest variation and sensitivity of the voltage on the buses among all the buses in the same region.

Next, a fuzzy controller is individually designed for each region which injects required reactive power into the region in case of disturbances and regional voltage variations. To act properly, the controller in each region needs a regional model. In order to obtain this model, an offline fuzzy learning algorithm is applied in each region and a nonlinear system model is estimated based on load disturbance inputs and bus voltage outputs.

Replacing conventional open-loop or centralized voltage control systems with intelligent decentralized control has many advantages such as: robustness, practical feasibility, ease of hardware implementation and low cost. Intelligent control such as fuzzy control has great advantages to solve nonlinear problems and to analyze the uncertain information associated with the model of system or process being controlled. In [21] a two layer fuzzy logic with hierarchical levels is described for control of regional as task-oriented control level and set-point control level. The high level control updates high-side voltage set points at power plants, and switches capacitor/reactor banks at the transmission network. The low level control is an automatic voltage regulator (AVR) at the power plants.

In this paper we use fuzzy rules to obtain a nonlinear model of system regions, and then fuzzy control is used to hold the buses voltage as close as possible to their regional reference values, especially useful when the power demand is heavy.

This is applied to IEEE-118 bus network with three regions and controllers installed on pilot buses in order to eliminate voltage violations in system. Therefore, the contribution of this paper is regulation of voltage by firstly finding the appropriate regions in the power network using graph theory, secondly finding the pilot buses in each region and finally designing a decentralized fuzzy controller for each region.

The paper is organized as follows: Section II presents the graph theory and partitioning algorithm. Section III describes pilot bus selection. Section IV demonstrates the model estimation achieved with a fuzzy algorithm. Section V presents the design of controllers with a fuzzy algorithm. Section VI presents the simulation results and finally we conclude in Section VII.

## II. Graph Partitioning Algorithm

### A. Graph Theory

The graph-partitioning problem involves a graph, $G=(V,\varepsilon)$ with vertices, $V=\nu_1,\nu_2,\dots,\nu_n$ and weighted edges where the weight of edge $e=(v_i,v_j)$ represents the cost of putting $\nu_i$ and $\nu_j$ in separate partitions.

The notion of weighted graphs, where each edge carries a cost, is fundamental to many applications of graph theory. We may associate to G a weight matrix $W$ that satisfies the following properties:

1) $\mathrm{w_{ij}} = \mathrm{w_{ji}}$.
2) $\mathrm{w_{ii}} = 0$.
3) $\mathrm{w_{ij}} \geq 0$ and $\omega_{\mathrm{ij}}=0$ if i is not adjacent to j in G.

The problem is to find a partition for the set of vertices $P=\{p_1,p_2,\dots,p_k\}$for a given $k$ that optimizes some cost criterion based on the weights of edges. Spectral-based partitioning extracts global information about the structure of a graph from eigenvalues/eigenvectors of graph matrices.

The relation between the properties of a graph and its spectrum are studied in [14]. The adjacency matrix of G is the $\mathrm{n}\times\mathrm{n}$ matrix $\mathrm{A(G)}=[a_{\mathrm{ij}}]$ where $\mathrm{a_{ij}}$ is the weight of the edge between $v_{\mathrm{i}}$ and $v_{\mathrm{j}}$. The degree matrix of G is the $\mathrm{n}\times\mathrm{n}$ matrix $\mathrm{D(G)}=[\mathrm{d_{ij}}]$ is defined by

$$d_{ij}=\begin{cases}\sum\limits_{k=1}^{n} a_{ik} & \text{if } i=j\\ 0 & \text{if } i\neq j.\end{cases} \tag{1}$$

The *Laplacian* of $G$ is the $n\times n$ symmetric matrix $L(G)=D(G)-A(G)$. Since the rows (and columns) sum to 0, the Laplacian is singular, it has rank at most $n-1$ and it has 0 as eigenvalue. The matrix $L(G)$ is positive semidefinite and has only real eigenvalues. Thus the smallest eigenvalue is 0 and all other eigenvalues are positive. The multiplicity of 0 as an eigenvalue represents the number of connected sub-graphs.

This section presents a spectral k-way partitioning formulation [14]. All $k$ partitions are found simultaneously using all the global information available in the eigenvectors. $\lambda_1,\lambda_2,\dots,\lambda_k$ are the $k$ smallest eigenvalues of the matrix $L$ and $x_1,x_2,\dots,x_k$ are the eigenvectors associated with eigenvalues from which the first eigenvectors partition vector will be built. The partition matrix $\hat{P}$ is defined as

$$\hat{P}=Z(X)XX^TZ(X) \tag{2}$$

where $Z(X)$ is a diagonal matrix with

$$z_{ij}=\frac{1}{\sqrt{\sum_{h=1}^{k} x_{ih}^{\prime 2}}}. \tag{3}$$

$\hat{P}_{ij}$ is the cosine of the angle between the two row vectors $i$ and $j$ and represents the closeness of vertices to each other. The first vertex is chosen at random and can be considered as center of the first region (for example vertex $c_1$). To find the second vertex, or the center of the second partition, $\hat{P}_{ic_1}$ *for* $i=1,\dots,n$ is calculated to find the minimum of $\hat{P}_{ic_1'}$, therefore the second center of the region is found. When searching other regions to find the $k$ region, the following equation is used:

$$\mathrm{Min\ Y}=\left(1-\hat{P}_{ic_1}\right)+\left(1-\hat{P}_{ic_2}\right)+\dots+\left(1-\hat{P}_{ic_k}\right). \tag{4}$$

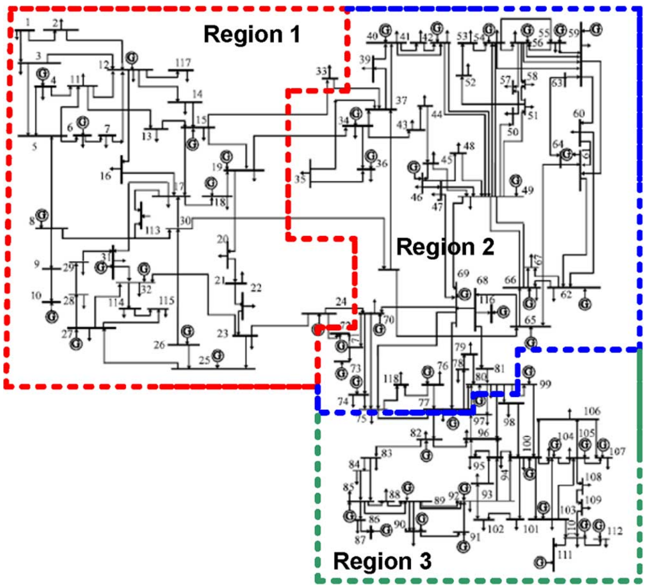


Fig. 1. Weighted partitioning (IEEE 118-bus network).

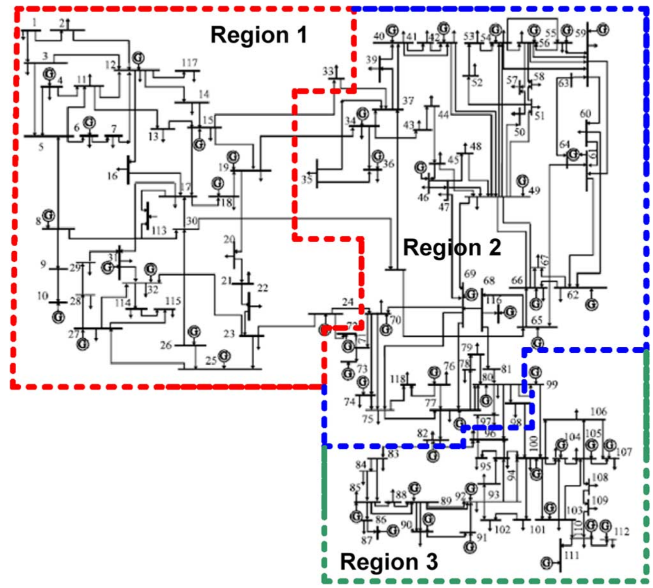


Fig. 2. Weighted partitioning (IEEE 118-bus network) after cutting some branches.

### *B. Case Study (IEEE 118-Bus Network)*

Here, the result of the graph partitioning algorithm is shown for the IEEE 118-bus network. After a number of tests have been performed, the number of regions is considered as three ($k = 3$). The result is compared with that of neural network partitioning algorithm presented in [22]. The comparison shows the effectiveness of the algorithm and the similarity of the obtained regions.

In the IEEE 118-bus network, there are 54 generators, 99 loads, 118 buses, and 186 branches (edges). The power flow has been obtained with the Matpower software [23].

Fig. 1 shows the result of partitioning when all weights are considered (apparent power between buses).

To check the robustness and performance of the partitioning algorithm based on graph theory for different operating conditions, two different tests have been performed.

1) Some of branches in regions have been opened to change the network structure and see the result of partitioning. Namely, branches between buses 4 and 11, 21 and 22 in region 1, branches between buses 35 and 36, 60 and 62 in region 2, branches between buses 82 and 83, 100 and 106 in region 3 have been opened. Fig. 2 shows the results of partitioning. Buses 82, 97 and 98 have move from region 3 to region 2. All other buses remain in their regions.
2) Disturbances are applied to ramp up all system loads simultaneously. The disturbances have been initiated at 5% and increased to 20%. The partitions stay approximately the same with some minor changes near the boundaries. Fig. 3 shows the result of partitioning when the load is increased by 10%. Compared to the partitioning in Fig. 1, buses 24 and 33 are moving to region 2 and bus 80 is moving to region 3.

## III. Pilot Bus Selection

In this section, the disturbances are applied separately to loads in each region of Fig. 1 to measure the interaction between regions and to check the buses voltage variations. This is instrumental to identify those buses with the highest sensitivity (pilot buses). In the following tables $v_{var}$ and $Q_{var}$ are calculated by the following equations:

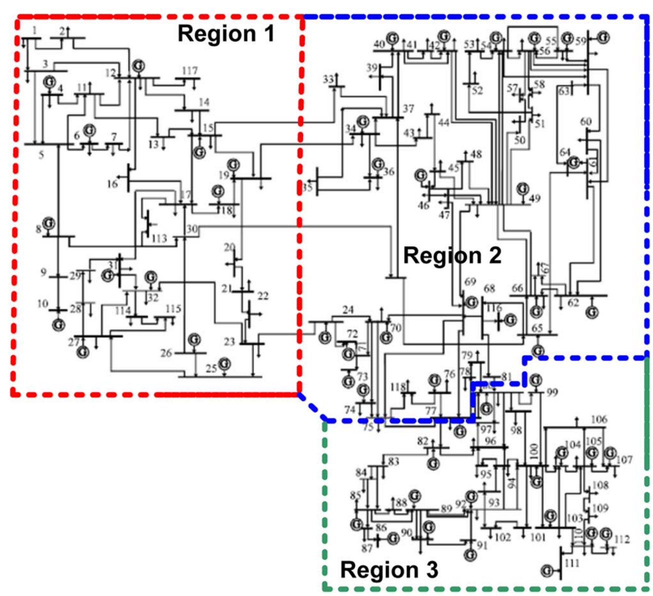


Fig. 3. Weighted partitioning (IEEE 118-bus network) after adding 10% disturbance to the loads.

$$v_{var}(\%) = \frac{\left|v_{ad(avg)} - v_{bd(avg)}\right|}{v_{bd(avg)}} \times 100 \tag{5}$$

$$Q_{var}(\%) = \frac{\left|Q_{ad(avg)} - Q_{bd(avg)}\right|}{Q_{bd(avg)}} \times 100 \tag{6}$$

where $v_{ad(avg)}$ and $Q_{ad(avg)}$ are, respectively, the average voltage of buses and the reactive power of generators in each region after disturbances applied to the loads while $v_{bd(avg)}$ and $Q_{bd(avg)}$ are the pre-disturbances values.

TABLE I
PERCENTAGE OF VOLTAGE VARIATIONS (DISTURBANCE IN REGION 1)

| IEEE 118_bus network | $v_{var}$(%) 5% $Dis$ | $v_{var}$(%) 10%$Dis$ | $v_{var}$(%) 20%$Dis$ |
|---|---|---|---|
| **Region** 1 | 0.0312 | 0.0640 | 0.1348 |
| **Region** 2 | 0.0073 | 0.0203 | 0.0486 |
| **Region** 3 | 0.0001 | 0.0002 | 0.0004 |

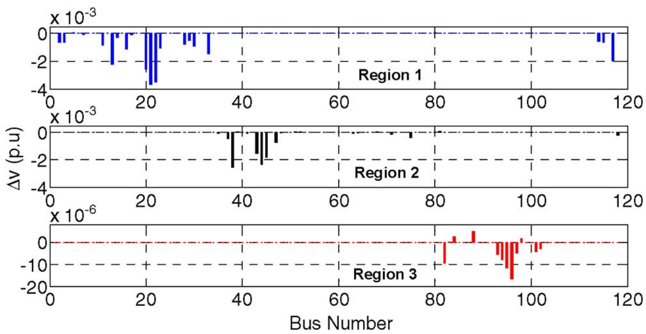


Fig. 4. Buses voltage difference in presence of disturbance in region 1 (IEEE 118-bus network).

TABLE II
PERCENTAGE OF REACTIVE POWER VARIATIONS (DISTURBANCE IN REGION 1)

| IEEE 118-bus network | $Q_{var}$(%) 5% $Dis$ | $Q_{var}$(%) 10% $Dis$ | $Q_{var}$(%) 20% $Dis$ |
|---|---|---|---|
| **Region** 1 | 3.24 | 8.1 | 18.2 |
| **Region** 2 | 2.19 | 4.57 | 10.03 |
| **Region** 3 | 0.27 | 0.28 | 0.29 |

In the first step, load disturbances are in region 1. This region has 21 buses and 16 generators and the percentage of generators to all buses is 43.2%.

Table I presents the percentage of buses voltage variations in each region.

As can be seen in this table, load disturbances in region 1 affect the voltages in this region more than that in other regions. This indicates that region 1 is adequately isolated from the two other regions.

Fig. 4 shows the buses voltage difference $([\Delta v = v]_{ad-v_{bd}})$ in presence of disturbances in region 1.

As illustrated, buses voltage in region 1 decrease more than voltages of the other regions. This confirms region 1 is separated from other regions.

Table II presents the percentage of the reactive power variations in each region for this event. It turns out that generators in region 1 produce more reactive power to regulate the voltage. Therefore in region 1 the generators are able to compensate against a drop in voltage. This explains why this region adequately isolated from the disturbances in other regions.

The results show buses 20, 21 and 22 are the most sensitive buses in this region and can be considered as pilot buses. Because these buses are close, bus 21 is considered as a main pilot bus in this region.

Next, load disturbances are applied in region 2. This region has 27 buses, 23 generators, and the percentage of generators to all buses is 46%. Table III presents the percentage of bus voltage variations in each region and shows that load disturbances in region 2 affects the voltages in this region more than that in other regions. Thus region 2 is adequately isolated from the two other regions.

TABLE III
PERCENTAGE OF VOLTAGE VARIATIONS (DISTURBANCE IN REGION 2)

| IEEE 118-bus network | $v_{var}$(%) 5% $Dis$ | $v_{var}$(%) 10%$Dis$ | $v_{var}$(%) 20%$Dis$ |
|---|---|---|---|
| **Region** 1 | 0.0038 | 0.0077 | 0.0162 |
| **Region** 2 | 0.0424 | 0.0861 | 0.1776 |
| **Region** 3 | 0.004 | 0.0003 | 0.0008 |

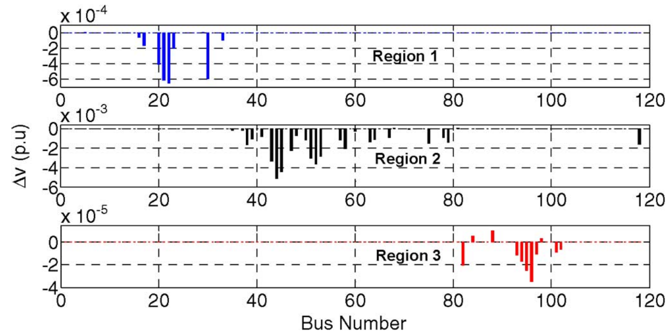


Fig. 5. Buses voltage difference in presence of disturbance in region 2 (IEEE 118-bus network).

TABLE IV
PERCENTAGE OF REACTIVE POWER VARIATIONS (DISTURBANCE IN REGION 2)

| IEEE 118-bus network | $Q_{var}$(%) 5% $Dis$ | $Q_{var}$(%) 10% $Dis$ | $Q_{var}$(%) 20% $Dis$ |
|---|---|---|---|
| **Region** 1 | 0.6 | 1.19 | 3.1 |
| **Region** 2 | 8.4 | 19.2 | 43 |
| **Region** 3 | 0.27 | 0.29 | 0.30 |

Fig. 5 shows $\Delta v$ in presence of disturbances in region 2. The buses voltage in this region decreases more than the ones in the other regions. This confirms that region 2 is adequately separated from other regions.

Table IV presents the percentage of reactive power variations in each region for this event.

As can be seen from this table, the generators in region 2 produce more reactive power to regulate the voltage. Therefore in region 2 the generators are able to compensate against a drop in voltage. This explains again why this region adequately isolated from the disturbances in other regions. The results show bus 44 is the most sensitive bus in this region and can be considered as the main pilot bus.

Finally, the disturbances are applied to the loads in region 3. This region has 16 buses, 15 generators and the percentage of generators to all buses is 48.4%. Table V presents the percentage of the buses voltage variations in each region. As can be seen in this table, load disturbances in region 3 affect the voltages in this region more than that in other regions. This indicates that region 3 is adequately isolated from the two other regions.

Fig. 6 shows $\Delta v$ for disturbances in region 3. The buses voltage in this region decreases more than the ones in other re-

TABLE V
PERCENTAGE OF VOLTAGE VARIATIONS (DISTURBANCE IN REGION 3)

| IEEE 118-bus network | $v_{var}(\%)$ 5% $Dis$ | $v_{var}(\%)$ 10% $Dis$ | $v_{var}(\%)$ 20% $Dis$ |
|---|---|---|---|
| **Region** 1 | 0.0001 | 0.0002 | 0.0005 |
| **Region** 2 | 0.0012 | 0.0027 | 0.0066 |
| **Region** 3 | 0.0348 | 0.0742 | 0.1674 |

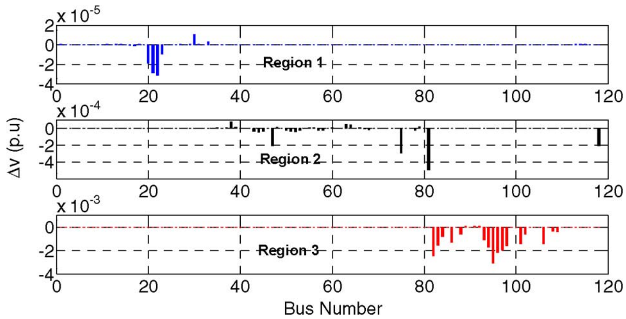


Fig. 6. Buses voltage difference in presence of disturbance in region 3 (IEEE 118-bus network).

TABLE VI
PERCENTAGE OF REACTIVE POWER VARIATIONS (DISTURBANCE IN REGION 3)

| IEEE 118-bus network | $Q_{var}(\%)$ 5% $Dis$ | $Q_{var}(\%)$ 10% $Dis$ | $Q_{var}(\%)$ 20% $Dis$ |
|---|---|---|---|
| **Region** 1 | 0.007 | 0.011 | 0.028 |
| **Region** 2 | 0.66 | 1.61 | 4.51 |
| **Region** 3 | 3.2 | 7.68 | 18.05 |

TABLE VII
PILOT BUSES (IEEE 118-BUS NETWORK)

| IEEE 118-bus network | Pilot Buses |
|---|---|
| **Region** 1 | 21,13,117,33,3 |
| **Region** 2 | 44, 52,47,75,118 |
| **Region** 3 | 95,82,98,106 |

gions. This confirms that region 3 is adequately separated from other regions.

Table VI presents the percentage of reactive power variations in each region for this event. It turns out that generators in region 3 produce more reactive power to regulate the voltage. Therefore in regions 3 the generators are also able to compensate against a drop in voltage and adequately isolated this region from the disturbances in other regions.

The results show bus 95 is the most sensitive bus in this region and can be considered as main pilot bus.

Table VII shows the pilot buses for the three regions of the IEEE 118-bus network.

## IV. GENERATION OF TRAINING DATA AND MODEL ESTIMATION

In this section, the generation of training data is explained. These are based on variations of active/reactive power on load buses as inputs and buses voltage measurement as outputs. The key idea is to construct a mapping between load disturbances

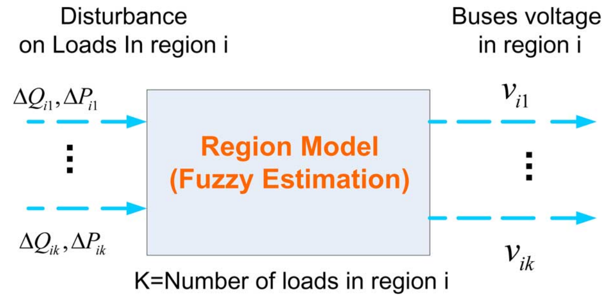


Fig. 7. Fuzzy region model estimation.

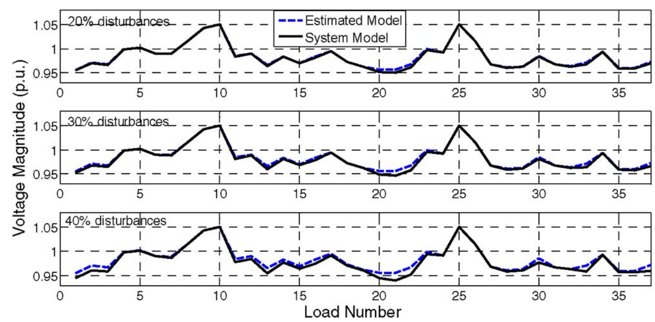


Fig. 8. System model and fuzzy model estimation for region 1.

and buses voltage in order to plan and carry out voltage regulation. The first step is the generation of the training data set.

Different sets of inputs and outputs are applied to obtain the nonlinear model of each region. For the first set of input/output data, disturbances have been added to all of the loads in the region. Then for the other set of input/output data, disturbances have been added randomly to different loads in the region to constitute sufficiently rich and meaningful data. After the training data set has been prepared, fuzzy rule antecedent membership functions have been identified by using the subtractive clustering algorithm. The consequent parameters of the rules are optimized by least square estimation (LSE). The subtractive clustering parameters that have been used for extracting the rules are: $radii = 0.4$, $squash\ factor = 0.4$, $accept\ ratio = 0.3$ *and* $reject\ ratio = 0.15$. With these parameters, a model with four fuzzy rules is identified. Fig. 7 shows the fuzzy system structure with desired inputs and outputs. The nonlinear model of each region is obtained using fuzzy model estimation.

Figs. 8–10 show the system and estimated model obtained by the fuzzy algorithm for each of the three regions separately.

As shown, after applying load disturbances in the regions, the error between the system and the estimated model increase. Table VIII presents the errors for each region separately. The error is calculated with the following equation:

$$\text{Error} = \frac{\sum_{i=1}^{k} V_{\text{system}}(i) - V_{\text{estimation}}(i)}{k} \tag{7}$$

where $k$ is number of load buses in the region.

Figs. 11 and 12 show the voltage of two representative pilot buses in regions 2 and 3, respectively. Inputs are chosen at random (they are variations of the loads reactive power).

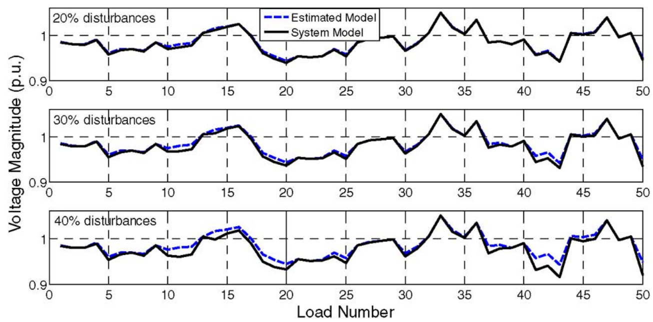


Fig. 9. System model and fuzzy model estimation for region 2.

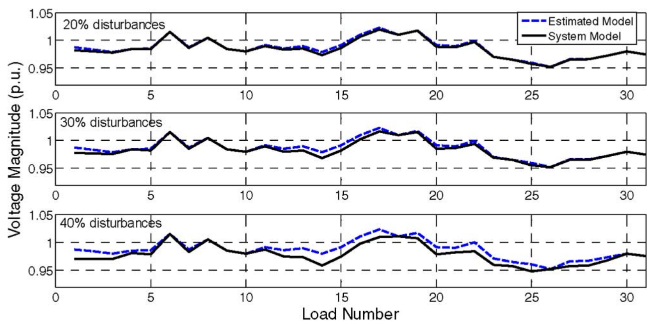


Fig. 10. System model and fuzzy model estimation for region 3.

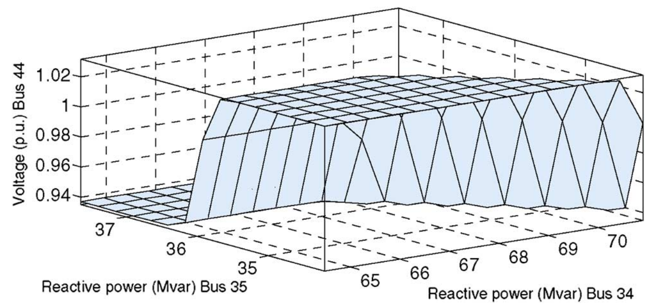


Fig. 11. Pilot bus voltage obtained by the fuzzy model and reactive power variations as inputs (region 2).

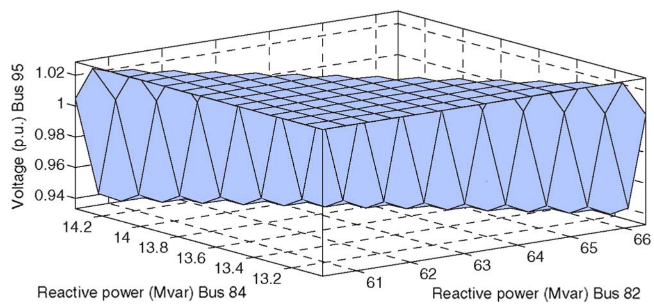


Fig. 12. Pilot bus voltage obtained by the fuzzy model and reactive power variations as inputs (region 3).

TABLE VIII
ERROR BETWEEN SYSTEM AND ESTIMATED MODEL

| IEEE 118-bus network | 20% Disturbance | 30% Disturbance | 40% Disturbance |
|---|---|---|---|
| Error Region 1 | 0.0010 | 0.0022 | 0.0045 |
| Error Region 2 | 0.0014 | 0.0034 | 0.0069 |
| Error Region 3 | 0.0016 | 0.0031 | 0.0080 |

## V. DECENTRALIZED FUZZY CONTROL DESIGN

Controls in each region are required to improve buses voltage when a disturbance occurs. This section addresses the design of controller at pilot buses through a fuzzy approach.

First the pilot buses are identified and represent the most sensitive point for SVC. The selection of pilot buses is based on the largest bus voltage variation and sensitivity among all the buses in the same region as explained in Section III. In practice, the pilot bus voltage are updated and coordinated considering the operating conditions.

Then decentralized controllers are designed separately for each region. This step requires a model of each region affected by interaction.

Fig. 13 presents the design of decentralized control in each region. The controller inputs are buses voltage variations in each region and its outputs are reactive power injected in pilot buses. If a region is affected by disturbances and the buses voltage approach their operating limits (especially on the pilot buses), the controller will check the ability of the generators in that region to provide the required reactive power and will supply it. If generators operate close to their limits, then the controller will adjoin control elements (inductors, capacitors, etc.) to the system to provide the needed reactive power to the region to prevent voltage violations.

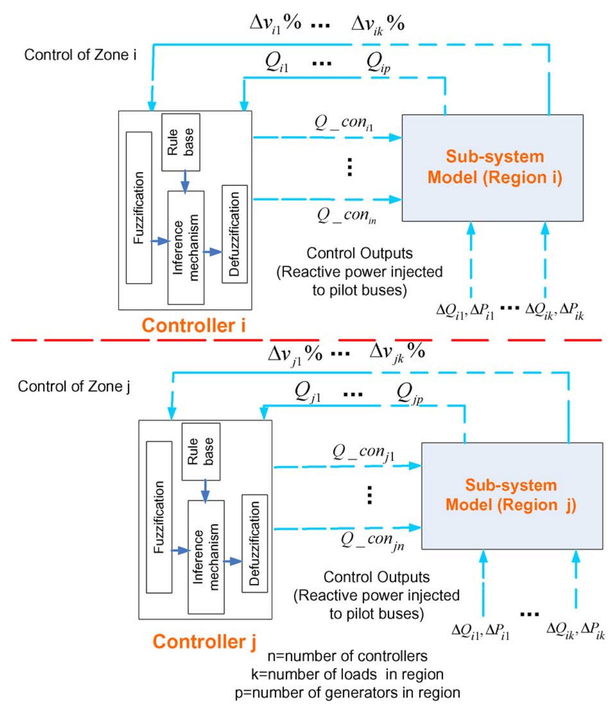


Fig. 13. Fuzzy control block diagram.

The control-law equations for voltage regulation are

$$\begin{bmatrix} Q_{con_{i1}} \\ \vdots \\ Q_{con_{in}} \end{bmatrix} = \begin{bmatrix} f_1(Q_{i1}, v_{i1}) \\ \vdots \\ f_n(Q_{ip}, v_{ik}) \end{bmatrix}. \tag{8}$$

TABLE IX
FUZZY TRAINING OUTPUTS FOR CONTROL OF REGION 1

| | Disturbances on Region 1 | | | | | | |
|---|---|---|---|---|---|---|---|
| | 10% | 20% | 25% | 30% | 35% | 40% | 50% |
| **Pilot Buses Region 1** | Reactive power injected to the pilot buses (MVar) | | | | | | |
| **21** | 0 | 0 | 2 | 4 | 6 | 10 | 12 |
| **13** | 0 | 0 | 0 | 0 | 2 | 6 | 10 |
| **117** | 0 | 0 | 0 | 0 | 2 | 4 | 5 |
| **33** | 0 | 0 | 0 | 0 | 0 | 3 | 8 |
| **3** | 0 | 0 | 0 | 0 | 0 | 0 | 8 |

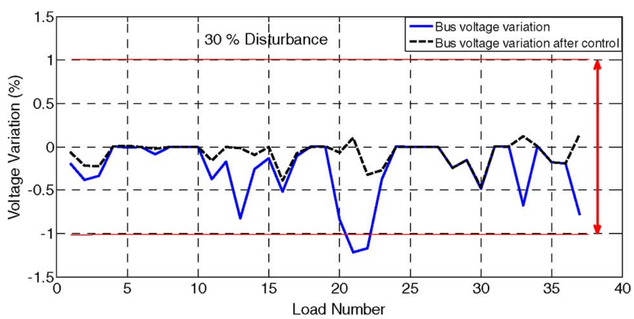


Fig. 14. Buses voltage before and after injection of reactive power to region 1 (30% disturbances).

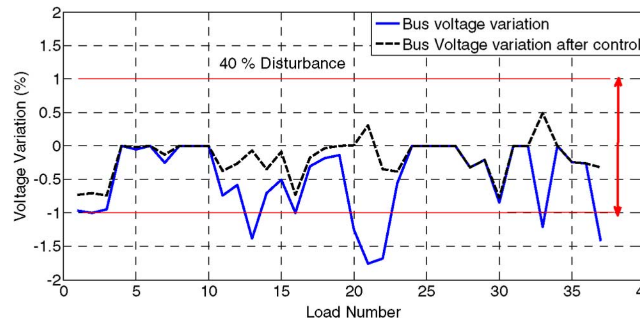


Fig. 15. Buses voltage before and after injection of reactive power to region 1 (40% disturbances).

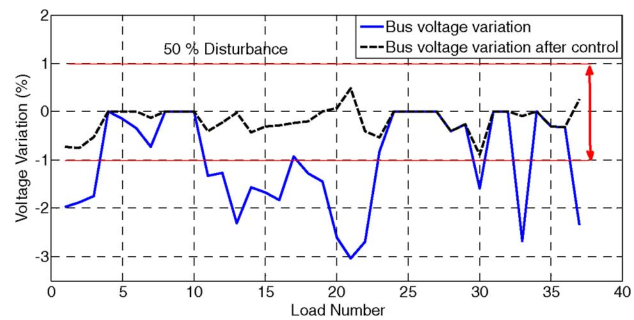


Fig. 16. Buses voltage before and after injection of reactive power to region 1 (50% disturbances).

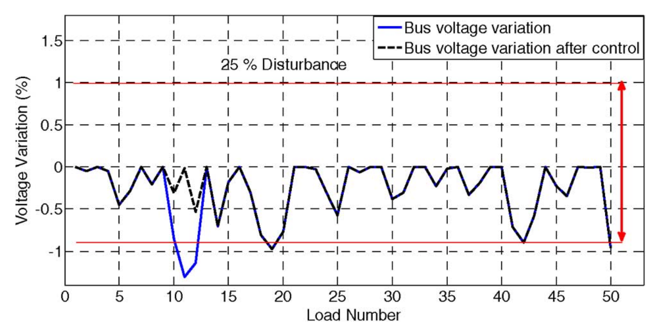


Fig. 17. Buses voltage before and after injection of reactive power to region 2 (25% disturbances).

The functions $f_1$ and $f_n$ are the control laws of a Sugeno-type fuzzy controller. Sugeno controllers take in fuzzy inputs and outputs. In this equation $v_{i1} \ldots v_{ik}$ are buses voltage in region, $Q_{con_{i1}} \ldots Q_{con_{in}}$ are reactive power injected into the region $i$ by controllers, and $Q_{i1} \ldots Q_{ip}$ are the reactive power generated by generators in region $i$. Table IX presents an example of the fuzzy training outputs for control of region 1. A similar training has been performed for regions 2 and 3, respectively. As can be seen in this table, the disturbances ranging from 10% to 50% are applied to the loads in this region and the reactive power is modified to prevent voltage violations.

## VI. Simulation Results

The simulation is to demonstrate the performance characteristics inferred from the theoretical development. A case study on the IEEE 118-bus network confirms the robustness and performance of the algorithm. In this section, we discuss the results of different tests on the IEEE 118-bus network. These tests are as follows:

1) Increase loads in each region individually, verify the voltage of the main pilot bus; when this voltage violates a limit then inject required power into the region;
2) Increase loads in each region individually, verify the voltage of the pilot buses; when this voltage violates a limit then inject required power into the region.

In the first test, 30% disturbances are applied to the loads in the region 1. Allowable variations on buses voltage are set to $\pm 1\%$. If buses voltage variations exceed 1%, the controller will modify reactive power to keep voltages in the desired ranges. Fig. 14 shows buses voltage in region 1 without and with controller.

As illustrated, the 30% disturbances cause voltage of pilot bus 21 to drop more than 1%. In this situation, reactive power is supplied at this pilot bus, bus voltage increases and stays within the desired voltage range. Next, disturbances are increased to 40% and 50%, respectively, and Figs. 15 and 16 show the buses voltage. As can be seen in these figures, the controller for pilot bus 21 is not sufficient to regulate the voltages and therefore, other controllers installed in pilot buses add reactive power to the region to compensate voltages drop. These controllers are installed in pilot buses 21, 13, 117, 33, and 3, respectively.

In the second test, the loads in the region 2 are increased to 25%. Fig. 17 shows buses voltage in region 2 without and with the controller.

The scenario cause voltage of pilot bus 44 drops under 1% of variation. In this situation, reactive power is added on this pilot bus and its bus voltage increases and stays within the allowable range. Next, disturbances are 32% and 40%, respectively, in Figs. 18 and 19. Here, the controller for pilot bus 44

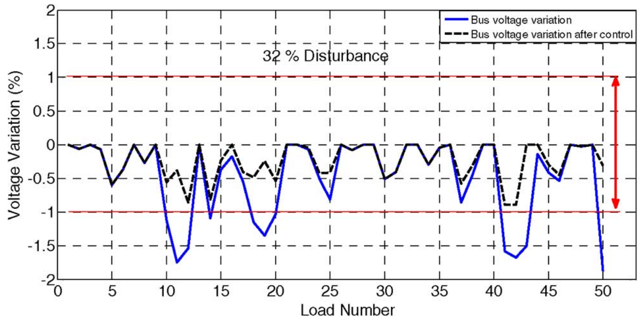


Fig. 18. Buses voltage before and after injection of reactive power to region 2 (32% disturbances).

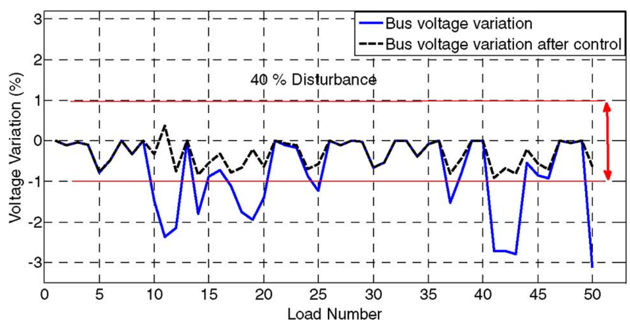


Fig. 19. Buses voltage before and after injection of reactive power to region 2 (40% disturbances).

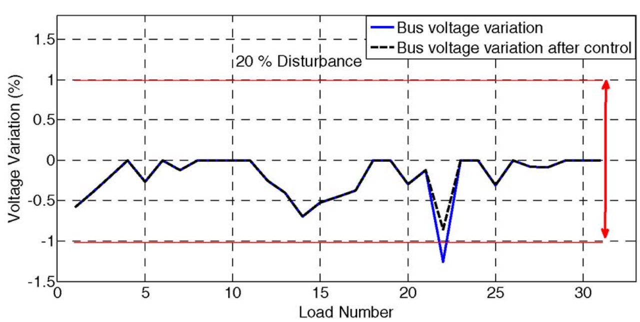


Fig. 20. Buses voltage before and after injection of reactive power to region 3 (20% disturbances).

is not enough to regulate the voltages and therefore, other controllers installed on pilot buses supply reactive power to the region. These controllers are installed at pilot buses 44, 52, 47, 75, and 118, respectively.

In the third test, the loads in the region 3 are increased by 20%. Fig. 20 shows the buses voltage in region 3 without and with the controller.

The scenario causes voltage of pilot bus 95 falls under its accepted range. In this situation, reactive power is added in this pilot bus, bus voltage increases and there is no violation.

Next, disturbances are increased to 30% and 40%, respectively, and Figs. 21 and 22 show the buses voltage. Here, the reactive power injected by the controller in pilot bus 95 is not enough to regulate the voltages and therefore other controllers come in. These controllers are installed at pilot buses 95, 82, 98, and 106, respectively.

## VII. Conclusion

Voltage control of power systems is essential as these systems operating closer to their limits. For practical reasons, researchers are becoming more and more interested in addressing this issue with secondary voltage control. In this paper, an electrical network graph partitioning technique was introduced to divide the system into regions. Graph theory plays an important role to simplify and split huge connected networks. Then pilot buses were selected in each region. Identification of pilot buses facilitates preventing the propagation of disturbances with decentralized controls. A fuzzy algorithm was presented to find an appropriate model of each region in order to design a proper controller.

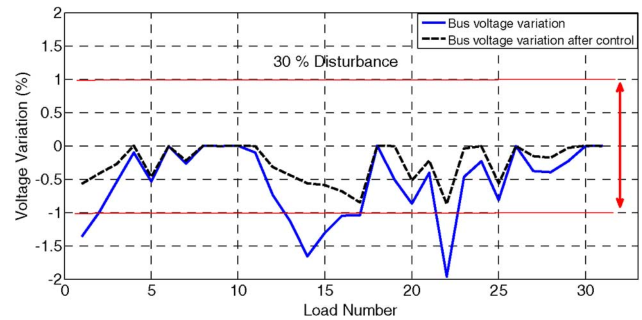


Fig. 21. Buses voltage before and after injection of reactive power to region 3 (30% disturbances).

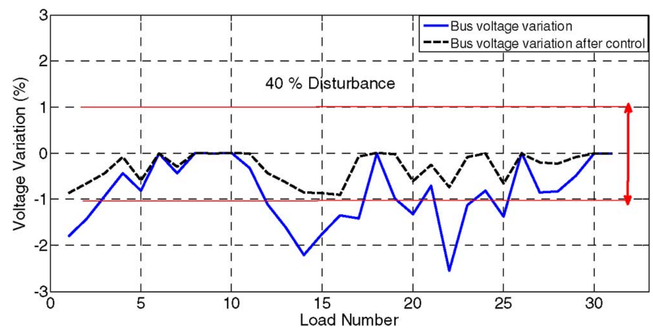


Fig. 22. Buses voltage before and after injection of reactive power to region 3 (40% disturbances).

The response of the fuzzy modeling and control shows the performance and robustness of the graph partitioning algorithm to prevent voltage violations in power system. The results illustrate that fuzzy decentralized control has the ability to cope with disturbances and minimize the interaction between regions.

The Research Institute of Hydro-Quebec (IREQ) has developed an optimal power flow based on tertiary voltage control algorithm for the Hydro-Quebec transmission system. The real-time function is able to solve the system at the same rate than the state estimator. This means that the control actions can be implemented every 5 minutes. There is also a regional voltage control that makes faster control actions, when necessary and in response to system disturbances. The goal is to use the existing supervisory control and data acquisition (SCADA) and wide area stability and voltage control system (WACS) as the communication and control infrastructure to achieve coordinated and automated voltage regulation.

## References

[1] J. P. Paul, J. Y. Leost, and J. M. Tesseron, "Survey of the secondary voltage control in France: Present realization and investigation," *IEEE Trans. Power Syst.*, vol. 2, no. 2, pp. 505–511, May 1987.

[2] P. Lagonotte, J. C. Sabonnadiere, J. Y. Leost, and J. P. Paul, “Structure analysis of the electrical system: Application to secondary voltage control in France,” *IEEE Trans. Power Syst.*, vol. 4, no. 2, pp. 479–486, May 1989.

[3] A. Stancovie’, M. Ili’c, and D. Maratukulam, “Recent results in secondary voltage control of power systems,” *IEEE Trans. Power Syst.*, vol. 6, no. 1, pp. 94–101, Feb. 1991.

[4] B. Marinescu and H. Bourles, “Robust predictive control for the flexible coordinated secondary voltage control of large-scale power systems,” *IEEE Trans. Power Syst.*, vol. 14, no. 4, pp. 1262–1268, Nov. 1999.

[5] S. Corsi, M. Pozzi, C. Sabelli, and A. Serrani, “The coordinated automatic voltage control of the Italian transmission grid—Part I: Reasons of the choice and overview of the consolidated hierarchical system,” *IEEE Trans. Power Syst.*, vol. 19, no. 4, pp. 1723–1732, Nov. 2004.

[6] S. Corsi, M. Pozzi, M. Sforna, and G. Dell’Olio, “The coordinated automatic voltage control of the Italian transmission grid—Part II: Control apparatuses and field performance of the consolidated hierarchical system,” *IEEE Trans. Power Syst.*, vol. 19, no. 4, pp. 1733–1741, Nov. 2004.

[7] M. Larsson, D. J. Hill, and G. Olsson, “Emergency voltage control using search and predictive control,” *Electr. Power Energy Syst.*, vol. 24, no. 2, pp. 121–130, Feb. 2002.

[8] J. Y. Wen, Q. H. Wu, D. R. Turner, S. J. Cheng, and J. Fitch, “Optimal coordinated voltage control for power system voltage stability,” *IEEE Trans. Power Syst.*, vol. 19, no. 2, pp. 1115–1122, May 2004.

[9] H. F. Wang, H. Li, and H. Chen, “Coordinated secondary voltage control to eliminate voltage violations in power system contingencies,” *IEEE Trans. Power Syst.*, vol. 18, no. 2, pp. 588–595, May 2003.

[10] Q. Wu, D. H. Popovic, D. J. Hill, and C. J. Parker, “Voltage security enhancement via coordinated control,” *IEEE Trans. Power Syst.*, vol. 16, no. 1, pp. 127–135, Feb. 2001.

[11] H. M. Ma, K. T. Ng, and K. F. Man, “Multiobjective coordinated power voltage control using jumping genes paradigm,” *IEEE Trans. Ind. Electron.*, vol. 55, no. 11, pp. 4075–4084, 2008.

[12] H. You, V. Vittal, and Z. Yang, “Self-healing in power systems: An approach using islanding and rate of frequency decline-based load shedding,” *IEEE Trans. Power Syst.*, vol. 18, no. 1, pp. 174–181, Feb. 2003.

[13] G. Xu and V. Vittal, “Slow coherency based cutset determination algorithm for large power systems,” *IEEE Trans. Power Syst.*, vol. 25, no. 2, pp. 877–884, May 2010.

[14] P. K. Chan, D. F. Schlag, and J. Y. Zien, “Spectral K-way ratio-cut partitioning and clustering,” *IEEE Trans. Comput. Aided Design Integr. Circuits Syst.*, vol. 11, no. 9, pp. 1088–1096, Sep. 1994.

[15] J. H. Chow*, Time-Scale Modelling of Dynamic Network With Applications to Power Systems*. New York: Springer-Verlag, 1982, vol. 46.

[16] M. Jonsson, M. Begovic, and J. Daalder, “A new method suitable for real-time generator coherency determination,” *IEEE Trans. Power Syst.*, vol. 19, no. 3, pp. 1473–1482, Aug. 2004.

[17] S.-K. Joo, C.-C. Liu, L. E. Jones, and J.-W. Choe, “Coherency and aggregation techniques incorporating rotor and voltage dynamics,” *IEEE Trans. Power Syst.*, vol. 19, pp. 1068–1075, 2004.

[18] E. De Tuglie, S. M. Iannone, and F. Torelli, “A coherency recognition based on structural decomposition procedure,” *IEEE Trans. Power Syst.*, vol. 23, pp. 555–563, 2008.

[19] A. Conejo and M. Aguilar, “A nonlinear approach to the selection of pilot buses for secondary voltage control,” *IEE Proc.—Power Syst. Control Manage.*, 1996.

[20] A. A. P. Lerm, “Using the bifurcation theory to select pilot busbars in a secondary voltage regulation scheme,” in *Proc. 2006 IEEE/PES Power Systems Conf. Expo.*, 2006, pp. 2096–2100.

[21] A. B. Marques, G. N. Taranto, and D. M. Falcao, “A knowledge-based system for supervision and control of regional voltage profile and security,” *IEEE Trans. Power Syst.*, vol. 20, no. 1, pp. 400–407, Feb. 2005.

[22] J. Mezquita, D. Asber, S. Lefebvre, M. Saad, and P. J. Lagacé, “Power network partitioning with a fuzzy C-means,” in *Proc. IASTED Int. Conf. Power and Energy Systems and Applications (PESA 2011)*, Pittsburgh, PA, Nov. 7–9, 2011.

[23] R. D. Zimmerman, C. E. Murillo-Sánchez, and R. J. Thomas, “MATPOWER: Steady-state operations, planning, and analysis tools for power systems research and education,” *IEEE Trans. Power Syst.*, vol. 26, no. 1, pp. 1088–1096, Feb. 2011.

**Hasan Mehrjerdi** received the B.Sc. and M.Sc. degrees in electrical engineering from Ferdowsi University of Mashhad, Mashhad, Iran, and Tarbiat Modares University, Tehran, Iran, respectively. He received the Ph.D. degree in electrical engineering from Quebec University (École de technologie supérieure), Montreal, QC, Canada in 2010.

He joined Power Systems And Mathematics Department at Research Institute of Hydro-Quebec (IREQ), Varennes, QC, Canada, in 2011. His current research interests are power system and coordination studies, integration of renewable energy resources, and smart grid.

**Serge Lefebvre** received the Bachelor and Master’s degrees in electrical engineering from the École Polytechnique, Montreal, QC, Canada, and the Ph.D. degree from Purdue University, West Lafayette, IN.

At the Research Institute of Hydro-Quebec (IREQ), he has been involved in the modeling and analysis of transmission and distribution systems. His current work involves energy and distribution management applications and he is actively involved in the evolution of the network towards a smart grid.

**Maarouf Saad** (SM’08) received the Bachelor and Master’s degrees in electrical engineering from École Polytechnique, Montreal, QC, Canada, in 1982 and 1984, respectively. In 1988, he received the Ph.D. degree in electrical engineering from McGill University.

He joined École de Technologie Supérieure in 1987, where he is teaching control theory. His research is mainly in nonlinear control and optimization applied to power systems, flight control, and robotics.

**Dalal Asber** received the B.Sc. degree in electrical engineering from the University of Damascus, Syria, in 1979 and the M.Sc. and Ph.D. degrees in automatic control from Institut National Polytechnique, Nancy, France, in 1988 and 1991, respectively.

After a postdoctoral position at École de Technologie Supérieure in Montreal, QC, Canada, she joined the Hydro-Quebec Research Institute (IREQ) in 1993, where she has been active in the areas of power system modeling, simulation, and control.